Supporting Information for

"Nanowire-Mediated Delivery Enables Functional Interrogation of Primary Immune Cells: Application to the Analysis of Chronic Lymphocytic Leukemia"

Alex K. Shalek,[1,*] Jellert T. Gaublomme,[1,*] Lili Wang,[3,4] Nir Yosef,[5] Nicolas Chevrier,[5] Mette S. Andersen,[2] Jacob T. Robinson,[1] Nathalie Pochet,[5] Donna Neuberg,[7] Rona S. Gertner,[1] Ido Amit,[5] Jennifer R. Brown,[3] Nir Hacohen,[5] Aviv Regev,[5,6] Catherine J. Wu,[3,4] and Hongkun Park[1,2†]

[1]Department of Chemistry and Chemical Biology and [2]Department of Physics, Harvard University, 12 Oxford Street, Cambridge, MA 02138, USA

[3]Department of Medicine, Harvard Medical School and [4]Cancer Vaccine Center and [7]Department of Biostatistics and Computational Biology, Dana-Farber Cancer Institute, Boston, MA 02115, USA

[5]Broad Institute of MIT and Harvard, 7 Cambridge Center, Cambridge, MA 02142, USA

[6]Howard Hughes Medical Institute, Department of Biology, Massachusetts Institute of Technology, Cambridge, MA 02140, USA

[*]These authors contributed equally to this work.

[†]To whom correspondence should be addressed: Hongkun_Park@harvard.edu

Materials and Methods

Nanowire fabrication, functionalization, and labeling

For most experiments, 4 x 4 mm substrates displaying etched vertical silicon nanowires (NWs) were fabricated, silanized, and then coated with biomolecules as previously described[1]. Any deviations are noted below.

Ordered arrays of NWs (Figure 1d) were made by defining NW sites with photolithography, depositing an aluminum etch mask, reactive ion etching (RIE), and then thermally oxidizing and thinning with RIE.

For NW labeling experiments, 3-mercaptopropyltrimethoxysilane was directly substituted for 3-aminopropyltrimethoxysilane (APTMS) (Figure 1b and d, Figure S2). Subsequently, samples were coated with 3 mL of an Alexa Fluor Maleimide (Invitrogen), prepared according to the manufacturer's recommendation. After 30 minutes, samples were washed thrice in distilled, sterile water, and blown dry. The day after plating, cells were incubated in media containing 1:500 dilution of either: CellMask (Invitrogen, Figure 1b), 1 Vybrant DiI (Invitrogen, Figure 1d), 10 mg/mL Fluorescein Diacetate (FDA, Invitrogen, Figure S2a), or 1 mg/mL Octadecyl Rhodamine B Chloride (r18) in absolute ethanol (Invitrogen, Figure S2b). After a minute, samples were rinsed through PBS and then imaged using an upright confocal microscope (Olympus). In some instances, dead nuclei were counterstained by incubating the cells with 2 μM EthD-1 (Invitrogen).

Primary mouse immune cell isolation and culture

6-8 week old female C57BL/6J mice were obtained from Jackson Laboratories, and bone marrow-derived dendritic cells (BMDCs) were generated as previously described[2]. To

isolate mouse primary immune cells, spleens were dissociated into single-cell suspensions by passage through a nylon mesh (BD Falcon). CD4+ T cells, B cells, natural killer (NK) cells, dendritic cells (DCs), and macrophages (MΦ) were enriched via MACS separation with CD4, CD19, DX5, CD11c, and CD11b MicroBeads (Miltenyi Biotec), respectively. Prior to plating, sorted cell suspensions were filtered twice through 40 um nylon mesh to remove clumps. When extracting DCs, spleens were treated with 1 mg/mL Collagenase D in complete media at 37^{o}C for 20 minutes prior to dissociation to reduce clumping and debris. All splenic cells were culture in BMDC media[2] without GM-CSF.

Primary Immune cells were plated at the following numbers per 4 x 4 mm sample: mouse B cells - 50,000; human B cells – 20,000; mouse BMDCs – 10,000; mouse and human DCs – 10,000; mouse and human MΦ – 10,000; mouse NK cells – 50,000; and, mouse and human T cells – 100,000.

Primary human B cell isolation and culture

Heparinized blood samples were obtained from normal donors and patients enrolled on clinical research protocols at the Dana-Farber Harvard Cancer Center (DFHCC) approved by the DFHCC Human Subjects Protection Committee, as previously reported[3]. Peripheral blood mononuclear cells (PBMC) were isolated by Ficoll/Hypaque density gradient centrifugation. Normal human B cells were immunomagnetically isolated with CD19 MicroBeads (Miltenyi Biotec). All B cells were cultured in media consisting of AIM-V media (Invitrogen) supplemented with 2 μg/mL IL-4 (R&D Systems), 5 μg/mL insulin (Invitrogen), and 50 μg/mL transferrin (Roche).

Delivery of biomolecules using silicon NWs

Cells were plated on top of NW substrates precoated with fluorescently labeled molecules as previously described[1]. The following day, the cells were cultured 1 μg/mL Hoechst for 30 minutes and dipped into a live-dead staining solution (below) consisting of 2 μM TO-PRO-3 and 50 nM Fluorescein Diacetate in PBS for one minute. After washing, delivery was assessed by confocally imaging samples at a height of 5 μm above the substrate's surface (Figure 1c and e, Figure S7 and S8).

Scanning Electron Microscope Analyses

Cells were prepared as previously described[1] 24 h after plating (Figure 1a, Figure 3a).

Live-Dead Cell Imaging

Half an hour prior to imaging, Hoechst dye was added to the samples at a final concentration of 1 μg/mL. Immediately prior to imaging, each substrate was rinsed in PBS and placed in a live-dead staining solution consisting of 2 μM EthD-1 (Invitrogen) and either 2 μM Calcein-AM (Invitrogen) or 50 nM FDA in PBS for one minute. After rinsing, each sample was imaged using an upright confocal microscope equipped with a scanning stage (Olympus, Prior). To ensure that each sample was captured in its entirety, our imaging field was raster-scanned across each substrate using built-in multi-area viewing software (FV10, Olympus). At each location, three color (excitation wavelengths: 405 nm, 488 nm, and 559 nm) epifluorescence-like confocal images were

captured by fully opening the system's pinhole. Each experimental condition and time point was repeated in triplicate. Values represent mean ± s.e.m.

Analysis of Live-Dead Cell Imaging

Stack of images comprising each sample was analyzed using Matlab. For each sample, the live cell count was calculated by identifying the number of nuclei bound within a Calcein AM or FDA positive cell that did not stain for EthD-1 while the total cell count was derived from the total number of nuclei, bound or unbound. To aid in counting adjacent cells with overlapping fluorescence profiles, histograms of nuclear size were fit with a constrained double Gaussian. Subsequently, nuclei were counted by binning using the fitted mean. Objects below half the mean were discarded as debris.

Live-Dead Cell Imaging Considerations

Importantly, independent samples were assayed at each time point; after 24 hours, samples that had been examined and returned to the incubator showed little to no live cells upon restaining and reimaging. This is could be due to toxicity associated with either light exposure, the chemical stains themselves, or the duration of imaging (performed in room temperature PBS).

Immunofluorescence Staining and Imaging

Staining for *LEF1* was performed as previously described[1] using antibodies purchased from Cell Signal (Figure S15). Image analysis was performed as described above.

Differences in CLL sample viability post-knockdown prevented direct quantification of the degree of protein change that occurred due to knockdown.

CellTiter-Glo viability assay

In some instances, cell survival was measured using a luminescence cell viability assay that quantifies the amount of ATP present (CellTiter-Glo, Promega, Madison, WI) as per the manufacturer's recommendations, save minor modifications. In brief, samples on NWs were first moved from 48-well to 96-well plates which contained 100µL of prewarmed culture media in each well and were allowed to cool to room temperature. Then, 100 µL of CellTiter-Glo reagent was added to each wells and the plate was mixed on an orbital shaker for 5 minutes. The total contents of the well (200µL) were then transferred to fresh opaque 96 well luminescence measurement plates. Plates were read using a luminometer (Perkin Elmer TopCount, Perkin Elmer, Waltham, MA). An ATP standard curve was freshly generated for each experiment. All the conditions were run in triplicate and the data is represented as mean +/- S.E.M. Patient specific changes to CLL-B cell viability that resulted from knockdown of *LEF1* were consistent across repeat experiments (Figure S16). Average NT siRNA viabilities for each sample are presented in Figure S24**.**

siRNA

siRNAs were obtained from either Qiagen or Dharmacon. A full list is presented below.. For all BMDC experiments, human B cell experiments and viability tests, 3 µL of a 100 µM siRNA solution was used. For the murine *ex vivo* cell tests, three different

concentrations of siRNA were tested: 100, 33, or 11 μM. Of the cell types tested, only the B cells showed a concentration dependent knockdown in the range tested. Transient transfection of C57BL/6 mouse embryonic fibroblasts (MEFs; from ATCC) was performed using either DharmaFECT 1 or 3 as per the manufacturer's instructions. For vimentin knockdowns, an equal parts mixture of all three siRNAs listed was used. siRNAs were obtained from either Qiagen or Dharmacon as follows:

Target	**siRNA**	**Species**	**Company**	**Part Number**
Control	ON-TARGET*plus* Non-Targeting Pool siRNA	Human (Hs, *Homo sapiens*) Mouse (Mm, *Mus musculus*)	Dharmacon	D-001810-10
Cyclophilin B (*Ppib*)	ON-TARGET*plus* Cyclophilin B Control Pool	Mm	Dharmacon	D-001820-20
Polo-like kinase 2 (*Plk2*)	Plk2 ON-TARGETplus SMARTpool	Mm	Dharmacon	L-040151-00-0020

Lymphoid Enhancer-Binding Factor 1 (*LEF1*)	LEF1 ON-TARGET*plus* SMARTpool	Hs	Dharmacon	L-015396-00-0020
T-cell activation RhoGTPase activating protein (*TAGAP)*	TAGAP ON-TARGET*plus* SMARTpool	Hs	Dharmacon	L-008711-01-0020
SP110 nuclear body protein (*SP110*)	SP110 ON-TARGET*plus* SMARTpool	Hs	Dharmacon	L-011875-00-0020
Centrosomal Protein 72kDa (*CEP72*)	CEP72 ON-TARGET*plus* SMARTpool	Hs	Dharmacon	L-020549-00-0020

Vimentin (*VIM*)	Hs_VIM_11 HP Validated siRNA	Hs	Qiagen	SI02655198
Vimentin (*VIM*)	Hs_VIM_4 HP Validated siRNA	Hs	Qiagen	SI00302190
Vimentin (*VIM*)	Hs_VIM_5 HP Validated siRNA	Hs	Qiagen	SI00302197
	AllStars Hs Cell Death siRNA	Hs	Qiagen	1027299

Quantitative real-time polymerase chain reaction (qRT-PCR)

NW substrates were removed from their original multiwell plates and, after being washed with PBS, placed into a 96-well plate. Subsequently, cells from each sample were lysed and their mRNA was extracted using a TurboCapture 96 mRNA kit (Qiagen). Next, cDNA was synthesized using a Sensiscript RT Kit (Qiagen). qRT-PCR was performed as previously described in either a 96[1] or a 384 well format[4]. Knockdown was measured by comparing each value to the average obtained for six or more control samples. Error bars represent standard error.

For experiments testing the effects of NWs with and without molecular coating on cell activation, certain cell types did not show measurable cytokine mRNA levels prior to stimulation. In such instances, a Ct value of 40 was assigned.

Primers used:

Mouse (Mm, *Mus musculus*):

Gene (Symbol)	**Ascension**	**Sequence (or part number)**
Glyceraldehyde 3-phosphate dehydrogenase (*Gapdh)*	NM_008084	Forward: ggcaaattcaacggcacagt Reverse: agatggtgatgggcttccc
Tumor necrosis factor (*TNF, TNF-α)*	NM_013693	Forward: ccctcacactcagatcatcttct Reverse: gctacgacgtgggctacag
Interferon gamma (*Ifng, IFN-γ)*	NM_008337	Forward: atctggaggaactggcaaaa Reverse: ttcaagacttcaaagagtctgaggta
Interferon alpha 4 (*Ifna4, IFN-a-4)*	NM_010510	Forward: agcctgtgtgatgcaggaa Reverse: ggcacagaggctgtgtttct
Interferon beta (*Ifnb, IFN-b)*	NM_010510	Forward: ctggcttccatcatgaacaa Reverse: agagggctgtggtggagaa
Chemokine (C-X-C motif) ligand 1 (*Cxcl1)*	NM_008176	Forward: ctgggattcacctcaagaacatc Reverse: cagggtcaaggcaagcctc
Chemokine (C-X-C motif) ligand 10 (*Cxcl10)*	NM_021274	Forward: gccgtcattttctgcctca Reverse: cgtccttgcgagagggatc
Polo-like kinase 2 (*Plk2)*	NM_152804	Forward: catcaccaccattcccact Reverse: tcgtaacactttgcaaatcca
Cyclophilin B (*Ppib)*	NM_011149	QT00169736 – Qiagen

Human (Hs, *Homo sapiens)*:

Gene (Symbol)	**Ascension**	**Sequence (or part number)**
Tumor necrosis factor (*TNF,*	NM_000594	QT01079561 – Qiagen

TNF-α)		
Lymphoid enhancer-binding factor 1 (*LEF1)*	NM_016269, NM_001130713, NM_001166119	QT00021133 - Qiagen
Lymphoid Enhancer-Binding Factor 1 (*LEF1*)	NM_016269, NM_001130713, NM_001166119	Forward: cacggaaagaaagacagctaca Reverse: tctcttcctcttcttttttcttacca
Lysozyme (*LYZ*)	NM_000239.2	Forward: tggttacaacacacgagctaca Reverse: tctgaaatatcccataatcagtgc
C-type lectin domain family 12 member A (*CLEC12A*)	NM_201623.3, NM_138337.5	Forward: cactcgtggtatgagagtggata Reverse: aagtcaggtgcgtttcttataacc
Wingless-type MMTV integration site family, member 10A (*WNT10A*)	NM_025216.2	Forward: atccacgcgagaatgagg Reverse: ccgcatgttctccatcact
G Protein Coupled Receptor 160 (*GPR160*)	NM_014373.2	Forward: ggaagatcatcagtcaaggaaga Reverse: gaagacctgctgaaatacacatga
Killer Cell Lectin-Like Receptor subfamily D, member 1 (*KLRD1, CD94*)	NM_002262.3, NM_007334.2, NM_001114396.1	Forward: gtgggagaatggctctgc Reverse: tttgtattaaaagtttcaaatgatgga
CD160 Antigen (*CD160*)	NM_007053.2	Forward: cctcactacatccgtgaactcc

		Reverse: ctgctggtatccttggcttc
SP110 nuclear body protein (*SP110*)	NM_001185015.1	Forward: CCTATGCCATACACAAGCCATT Reverse: CCTCTCCAGTTGGGTGAGAAT
Centrosomal Protein 72kDa (*CEP72*)	NM_018140.3	Forward: CTCTCGCGCAACTCCTTGG Reverse: GTGGAGCCGAAACACTTCTG
T-cell activation RhoGTPase activating protein (*TAGAP)*	NM_054114.3	Forward: CCCAACCTCCTGCTACTCAA Reverse: GTCCTTCTGGGCTTCAAATG
Glyceraldehyde 3-phosphate dehydrogenase (*GAPDH)*	NM_001256799.1	QT00079247 - Qiagen

Nanostring Analysis

Expression levels for a 300 gene inflammatory and antiviral signature[2, 4] were examined in BMDCs plated on either glass, NWs, or NWs coated with NT siRNA, both in the presence and absence of a 4h LPS stimulation, as previously described[2, 4, 5]. The averages of two independent samples were plotted against one another using Matlab. 95% confidence intervals were computed by fitting a histogram built from the ratios of one sample's expression to its corresponding replicate over all conditions and genes (Figure

2d). **Expression values for each gene, normalized to the total sum of counts for a sample, are presented in Table S1.**

Microarray data analysis, ANOVA, and clinical considerations

Total RNA was isolated from CLL cells (>95% $CD19^{+}CD5^{+}$) using TRIzol reagent (Invitrogen), followed by column purification (RNeasy Mini Kit, Qiagen, Valencia CA). RNA samples were hybridized to Affymetrix U133A+ 2.0 arrays (Santa Cruz, CA) at the DFCI Microarray Core Facility. All expression profiles were processed using RMA, implemented by the ExpressionFileCreator module in GenePattern[6, 7] and Affymetrix probes were collapsed to unique genes (Gene Symbol) by selecting the probe with the maximal average expression for each gene. Batch effects were removed using ComBat[8], implemented by the ComBat module in GenePattern[7]. These microarray data can be accessed at http://www.ncbi.nlm.nih.gov/geo/info/linking.html with accession number GSE31048.

Wnt Pathway member (compiled from: http://www.stanford.edu/group/nusselab/cgi-bin/wnt/; http://www.sabiosciences.com/rt_pcr_product/HTML/PAHS-043A.html; refs. [9-11]) expression was globally (43%, 56 of 131 genes) dysregulated in the 193 CLL-B cell microarray samples relative to the 23 Normal donor controls (Figure S14) ($p < 0.05$; two-tailed Student's T-Test). Among these, LEF1 was the most significantly dysregulated ($p = 1.78E-37$). Despite considerable effort, we were unable to find a WNT pathway expression signature that correlated well with TTFT.

Genes significantly dysregulated between the three classes were identified using a one-way ANOVA (see Table S1). These 823 genes identified as significantly different

between classes were analyzed using DAVID or GSEA[12, 13]. This differentiating gene signature was subsequently used to classify 181 additional CLL patients as follows: (1) the Pearson correlation between each new patient and our 12 original samples was computed over the 823 ANOVA genes using z-scored expression data – z-scoring was performed to better weight each individual gene; (2) the average correlation for each new patient over the three groups was computed; and, (3) new samples were assigned to the response class to which they showed highest average correlation. Samples were deemed unclassifiable if their average correlation value was lower than the highest average cross-correlation observed between any of the original 12 samples and the other two groups. Notably, reducing this requirement and assigning based upon highest average correlation alone still yielded a Kaplan Meier plot with three significantly different traces ($p = 0.0106$, Logrank, Figure S23), without any significantly enriched cytogenetic features (see Table S3). Finally, pursuing that sample analysis using a non-parametric ANOVA (Kruskal-Wallis) resulted in an 800-gene signature (547 gene overlap with the ANOVA list) and also yielded a significant Kaplan Meier curve with similar ability to classify additional CLL-B cell patients.

The three original groups of four microarray samples, as well as the larger correlated classes and the groups assigned based on knockdown, were compared for significant differences in the presence of known cytogenetic factors[3, 14] using 3x2 Fisher Exact tests in StataSE 10. Expression profiles were plotted using GENE-E (http://www.broadinstitute.org/cancer/software/GENE-E/) or custom Matlab scripts. Data analysis, unless otherwise specified, was performed using Matlab.

We used a "single sample" extension of gene set enrichment analysis (SS-GSEA) implemented in R[15] to test the intersection of either all annotated gene sets or those previously reported as stem cell gene sets[16-18] and our ANOVA genes for differences in expression between our three response classes (see Table S2). Notably, the original 12 samples and extended classes showed enrichment for similar annotations, with the extended classes providing increase statistical power.

Additional statistical considerations.

Significances for the anti-survival effects of knocking down core WNT pathway members in either CLL or Normal B cells relative to a non-targeting control siRNA were calculated using Wilcoxon signed rank tests. Normal and CLL B cells, meanwhile, were comparing using a Mann-Whitney rank sum test. Tests were performed using Stata SE or Matlab.

Activation of immune cells

Unless otherwise specified, cells were stimulated for 4 h the day after being plated. Stimulation molecules and concentrations per sample were:

Cell Type	Molecule
Mm BMDCs	100 ng/mL LPS
Mm B Cells	100 ng/mL LPS and 25 ng/mL Mm IL-4
Mm DC Cells	100 ng/mL LPS
Mm MF Cells	100 ng/mL LPS
Mm NK Cells	20 ng/mL Mm IL-12 and 5 ng/mL Mm IL-18

Mm T Cells	10 mL Mm aCD3/CD28 Dynabeads and 1 ng/mL Mm IL-2
Hs B Cells	10 ng/mL IL-4 and 0.5 mg/mL Hs CD 40L

Ultra-pure *E. coli* K12 LPS was obtained from Invivogen; Hs CD 40L, Mm IL-4, Mm IL-12, and Mm IL-18 were obtained from R & D systems; Mm IL-2 and aCD3/CD28 DynaBeads were obtained from Invitrogen.

For human B cells plated on either glass or NWs, whether left bare or coated with siRNA, *TNF-α* transcript levels were equally high when stimulated with IL-4 and CD40L and similarly low in the absence of this activating stimulus.

Statistical considerations.

Significances for the anti-survival effects of knocking down core WNT pathway members in either CLL or Normal B cells relative to a non-targeting control siRNA were calculated using Wilcoxon signed rank tests. Normal and CLL B cells, meanwhile, were comparing using a Mann-Whitney rank sum test. Tests were performed using Stata SE or Matlab.

Supporting Figures

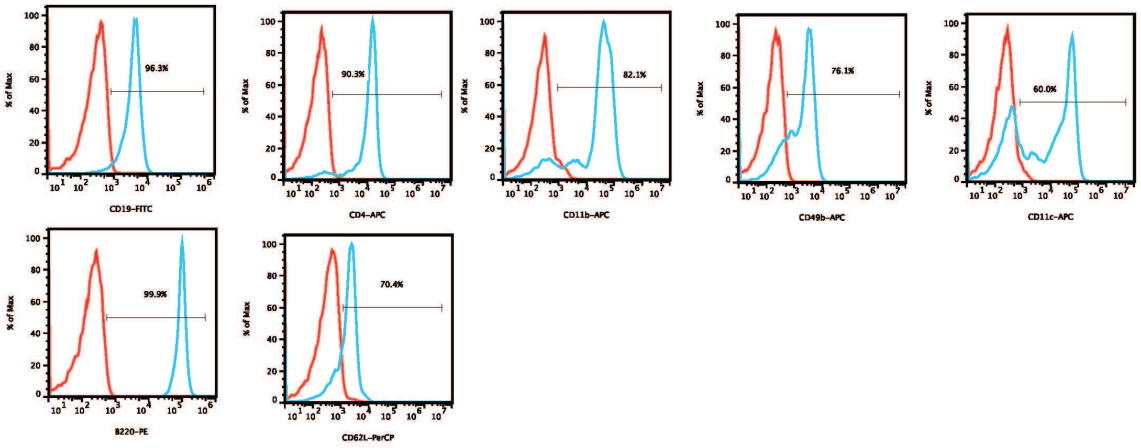

Figure S1. FACs data showing the purity of MACS-sorted mouse splenic cells used for the *ex vivo* experiments. For each plot, blue lines show the fraction of sorted cells staining positive while red show unstained controls. Cells were stained with fluorescently labeled antibodies (Miltenyi Biotech) according to the manufacturer's recommendations.

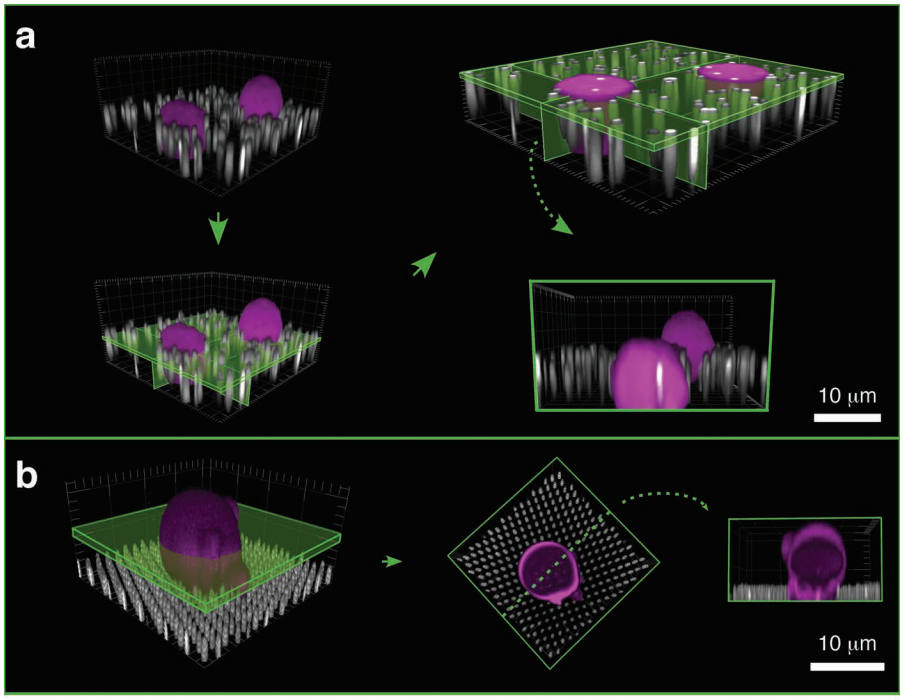

Figure S2. Long, sparse NWs penetrate the membranes of primary human B cells, while short, dense ones do not. (a) Human B cells (labeled with fluorescein diacetate (intact cytoplasm, magenta)) on long, sparse NWs labeled with Alexa 647 (white). Top Left: cross-section showing the location of the NWs within the cell. Bottom Left: Orthogonal view the highlighted XZ plane. Top Right: Orthogonal view of the other highlighted plane (YZ). (b) Human B cells (labeled with DiI (intact membranes, magenta)) on short, dense NWs labeled with Alexa 488 (white).

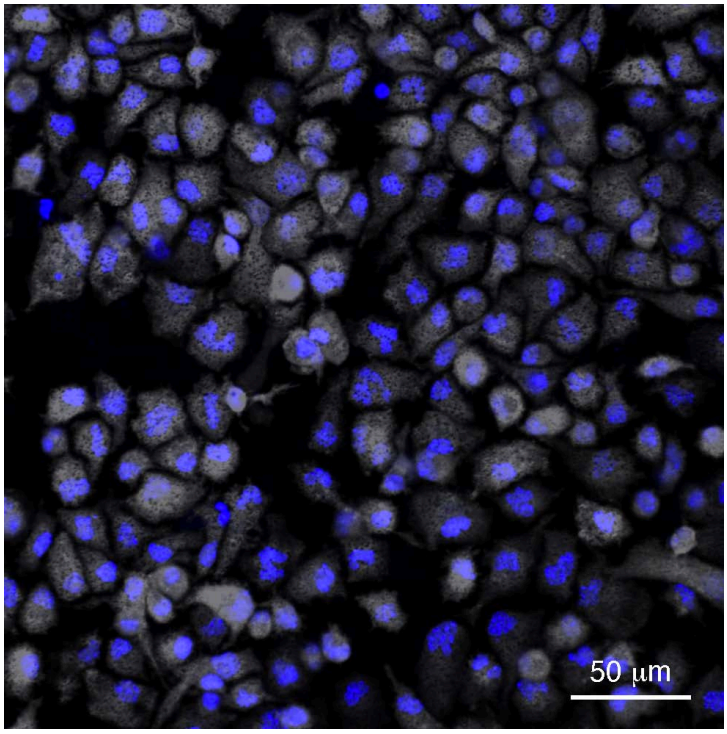

Figure S3. BMDCs, cytoplasms stained with fluoresecein diacetate (FDA, white) and nuclei counterstained with Hoechst (blue), plated on sharp, long (3 μm) NWs. In addition to showing disrupted cytoplasms at the sites of penetration (fluorescence voids), BMDCs on long SiNWs display pocked, irregularly shaped nuclei and decreased viability.

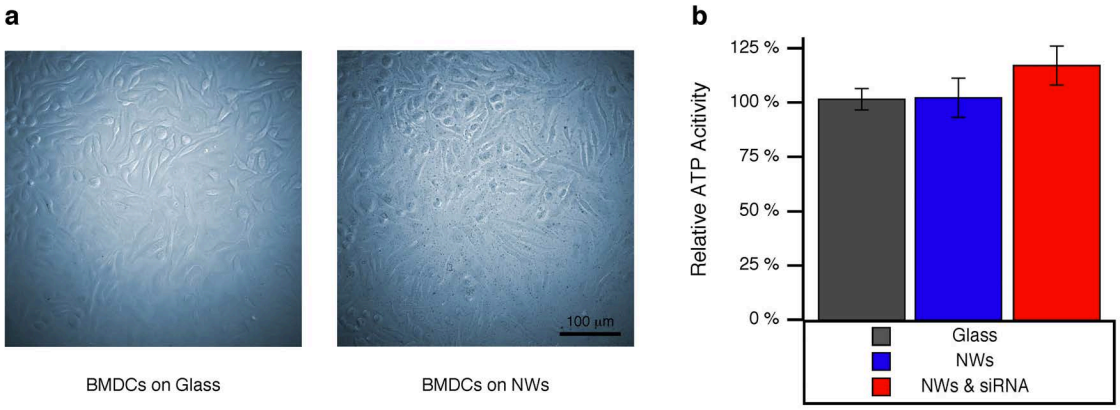

Figure S4. Optimized NWs do not affect BMDC viability. (a) Bright-field micrographs of BMDCs on either glass (left) or NWs (right) 24 hours after plating. (b) BMDC viability based on ATP activity (n = 3) after a 48-hour culture on glass, NWs or siRNA-coated NWs.

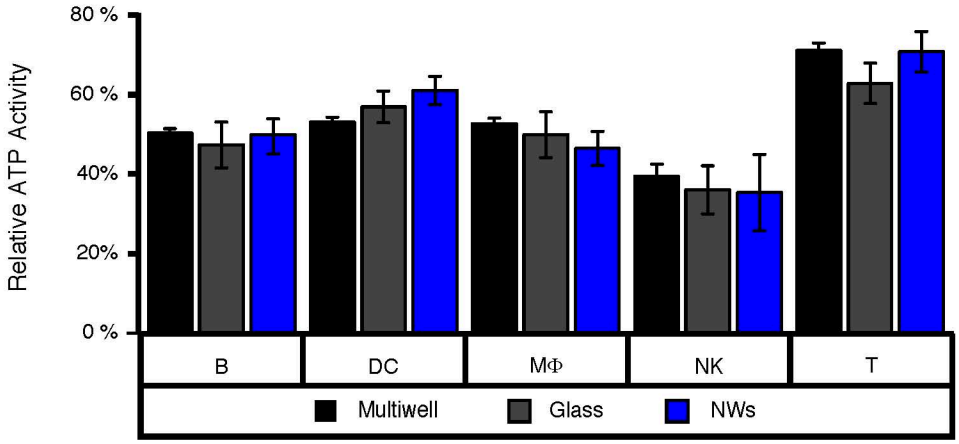

Figure S5. Optimized NWs do not adversely affect primary mouse splenocyte viability. Cells plated on flats (grey) and NWs (blue) show similar viability to cells plated in traditional tissue culture plates (n = 3).

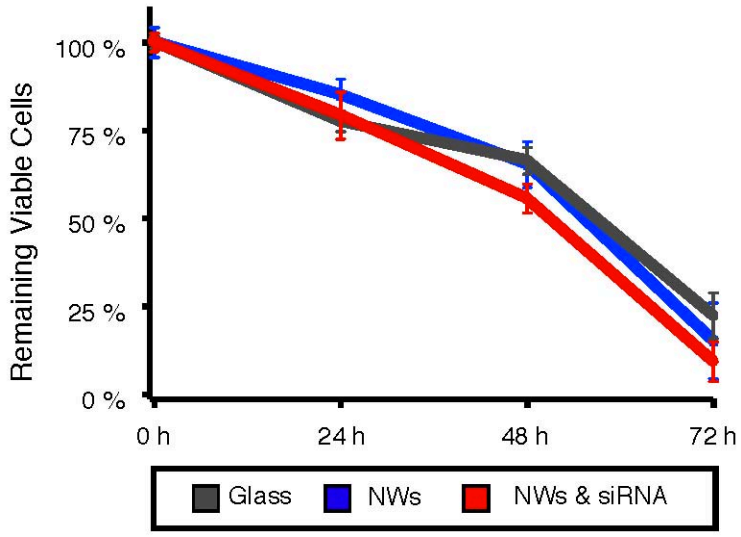

Figure S6. Neither NWs nor their cargo adversely affecting their viability. Viability (by imaging) over time for B cells plated on either flats (grey), NWs (blue), or siRNA-coated NWs (red). Values are mean ± standard error, n = 3

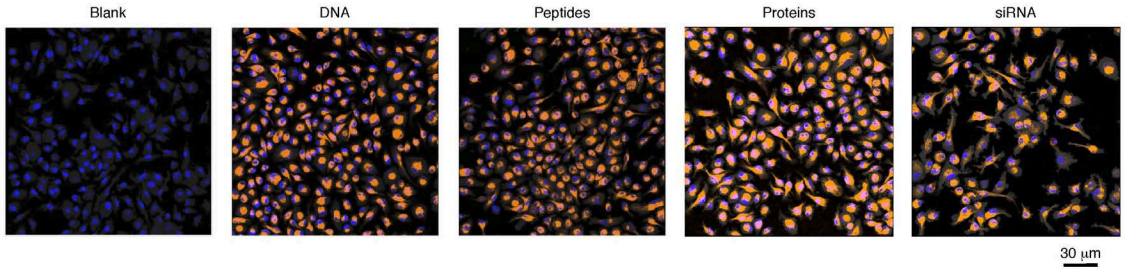

Figure S7. NWs can delivery a broad range of exogenous materials into BMDCs, a model primary immune cell. Confocal scans showing delivery of labeled molecules (orange) to BMDCs (intact membranes, grey; nuclei, blue) DNA: Cy3-pTRFP; Peptide: Rhodamine-labeled 7mer; Protein: Alexa 546-labeled Goat Anti-Chicken IgG; siRNA: Alexa 546-labeled Human Anti-Vimentin siRNA.

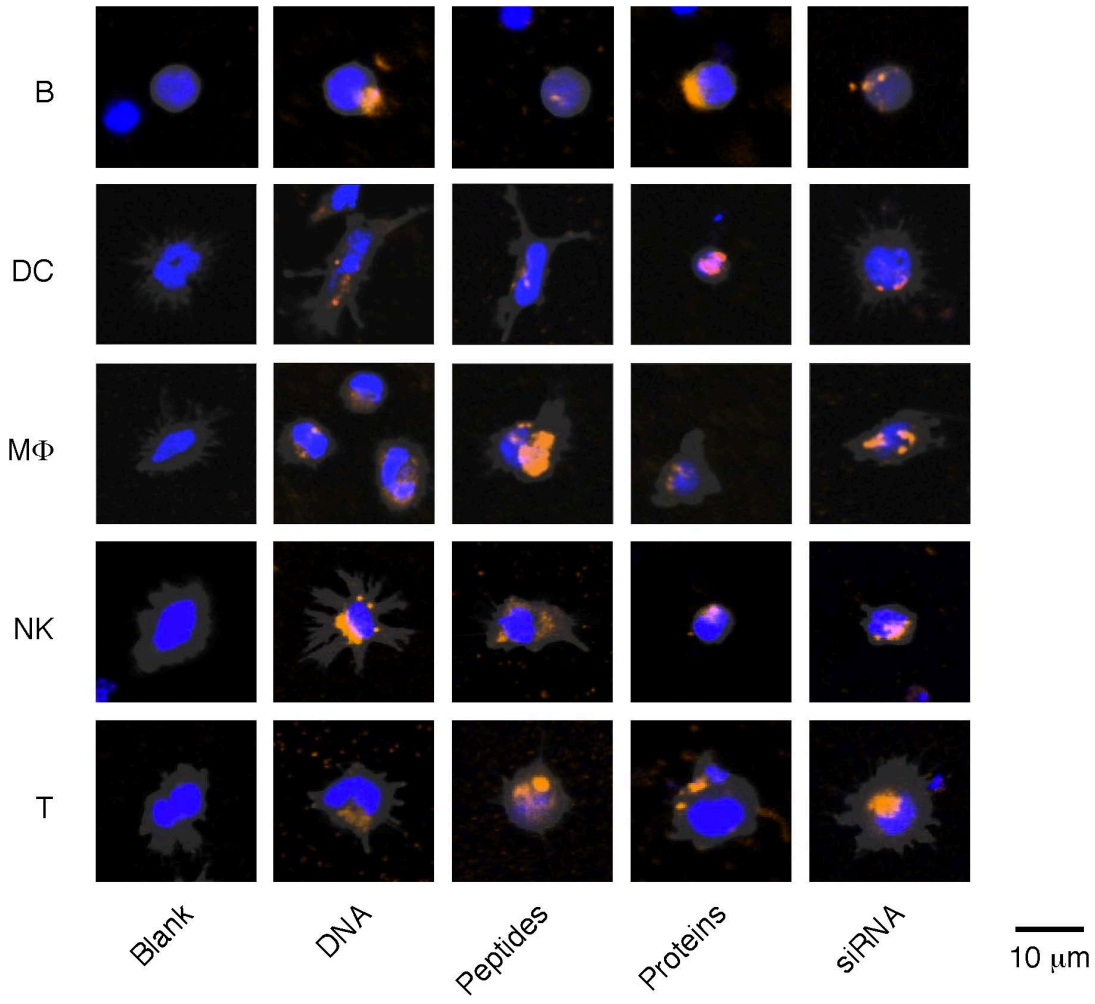

Figure S8. NWs can deliver a broad range of exogenous biomolecules into primary murine splenocytes. Confocal scans of labeled molecules (orange) delivered *ex-vivo* by NWs to mouse immune cells (FDA, grey; DAPI, blue). DNA: Cy3-pTRFP; Peptide: Rhodamine-labeled 7mer; Protein: Alexa 546-labeled Goat Anti-Chicken IgG; siRNA: Alexa 546-labeled Hs Anti-Vimentin siRNA.

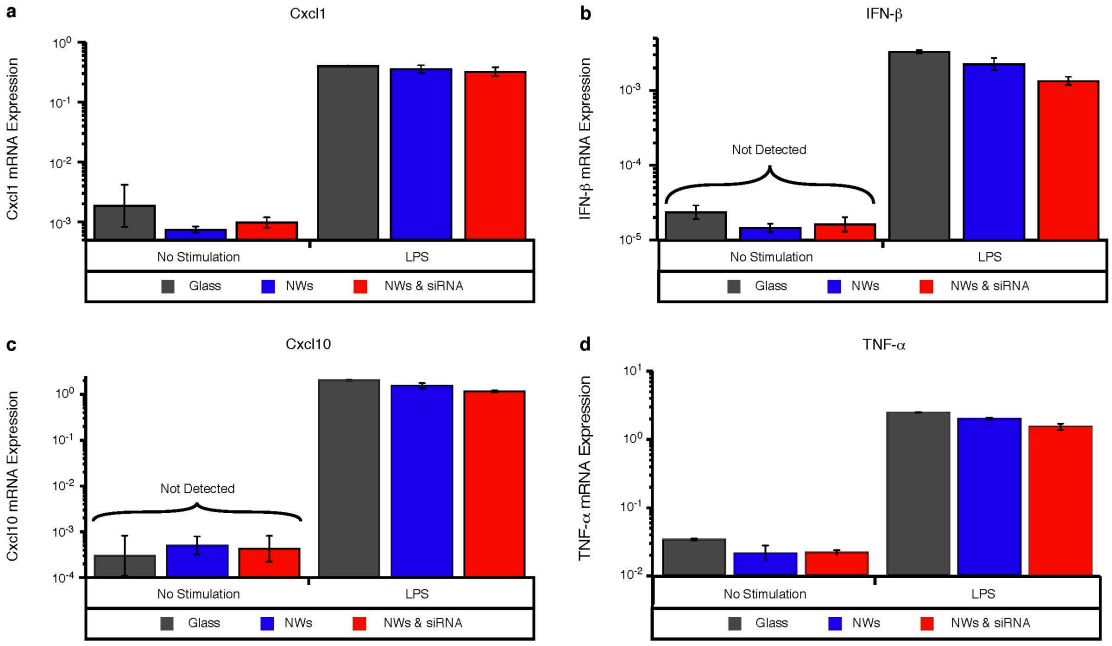

Figure S9. NWs and their cargo do not activate innate immune sensing or inhibit normal LPS induced responses. Whether plated on glass or NWs (with or without siRNA), BMDCs do not show detectable levels of *Cxcl1*, *Cxcl10*, *Ifn-β*, and *Tnf-α* in the absence of stimulation, suggesting that neither the NWs nor their cargo strongly activate the endogenous antiviral or inflammatory pathways in these cells. Similarly, when stimulated with LPS, *Cxcl1*, *Cxcl10*, *Ifn-β*, and *Tnf-α* are robustly induced to equivalent levels for all of the samples. *Ifnα4* was also undetectable for all sample types prior to stimulation. Y-axis: log scale; n = 3.

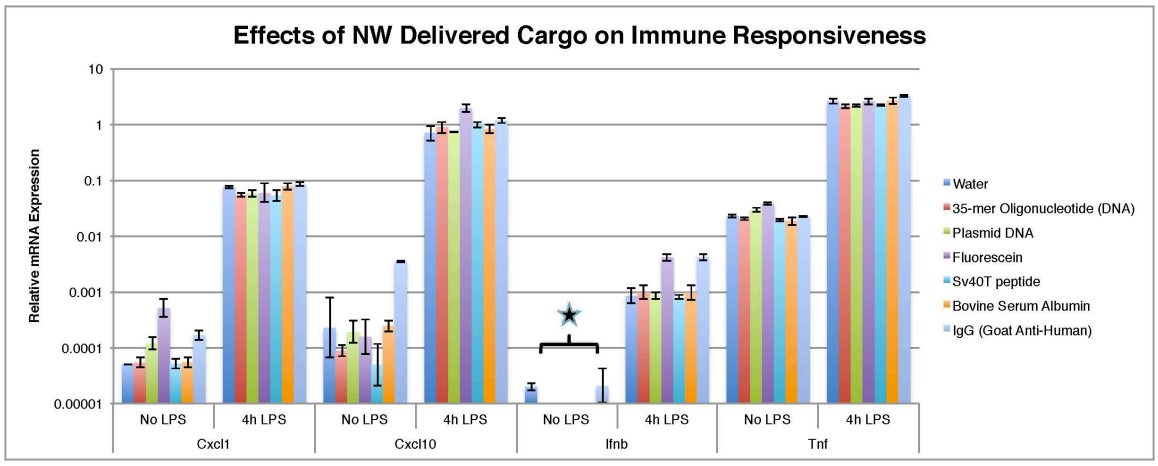

Figure S10. NWs and their cargo do not activate innate immune sensing or inhibit normal LPS induced responses. Just as with siRNA, oligonucleotides, plasmid DNA, small molecules, peptides, and proteins neither activate nor inhibit innate immune responses in BMDCs. ★ = transcript not detected. Error bars are S.E.M. for n = 3.

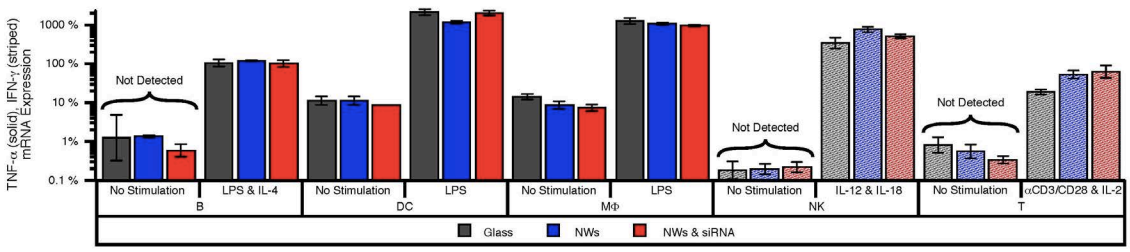

Figure S11. NWs and their cargo do not induce innate immune responses in primary splenocytes or inhibit their induction in the presence of conventional stimuli. Plating on bare or siRNA-coated NWs neither activates nor prevents activation of *ex vivo* immune cells, as measured by *Tnf-α* (B, DC, MΦ; solid bars) or *Ifn-γ* expression (NK, T; striped). Y-axis: log scale, n = 3. Relative expression for undetected transcripts was computed by assigning a Ct value of 40. All values are mean ± standard error.

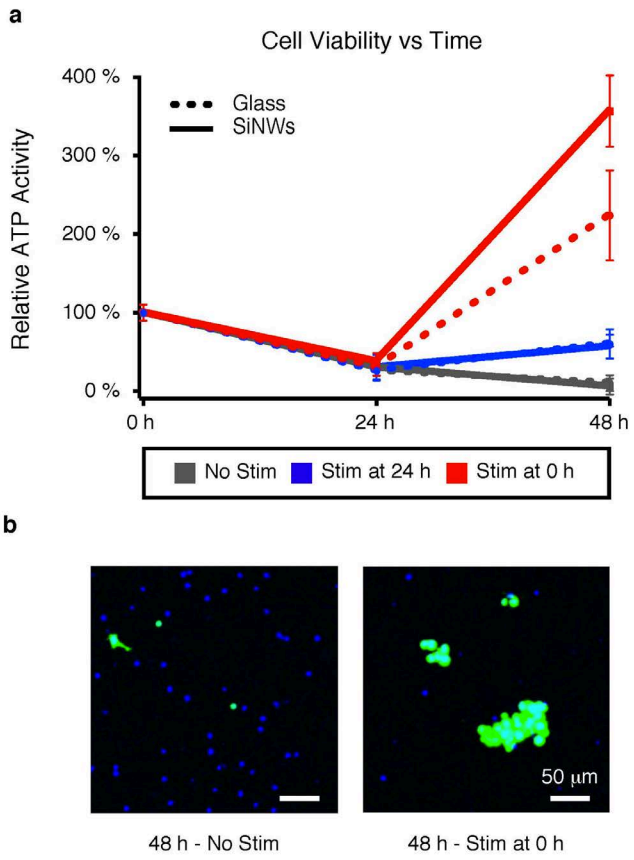

Figure S12. Stimulated mouse T cells grow and divide on NWs. (a) Whether on glass (dashed line) or NWs (solid line), unstimulated mouse T cells (grey) die off in culture. Addition of Il-2 and anti-$Cd3/_{Cd28}$ Dynabeads either immediately (red) or a day after plating (blue) results in activation and expansion. (b) When imaged, expansion is evident due to the appearance of large clusters of T cells on stimulated samples (right) as compared to unstimulated ones (left). Green, intact membranes (fluorescein diacetate); Blue, nuclei (Hoechst).

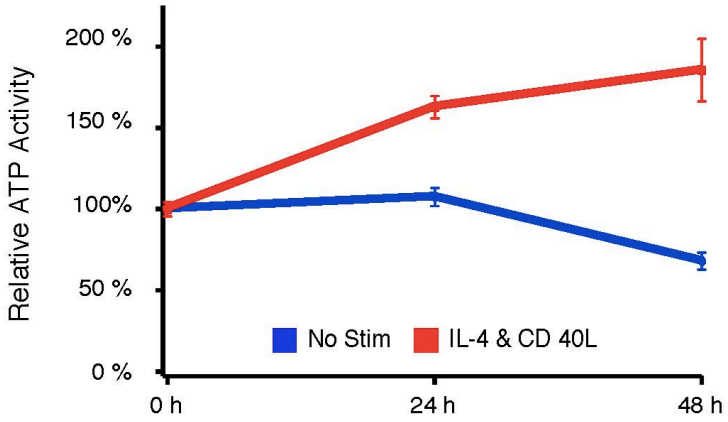

Figure S13. Human B cells will grow and divide on NWs when stimulated with IL-4 and CD40L.

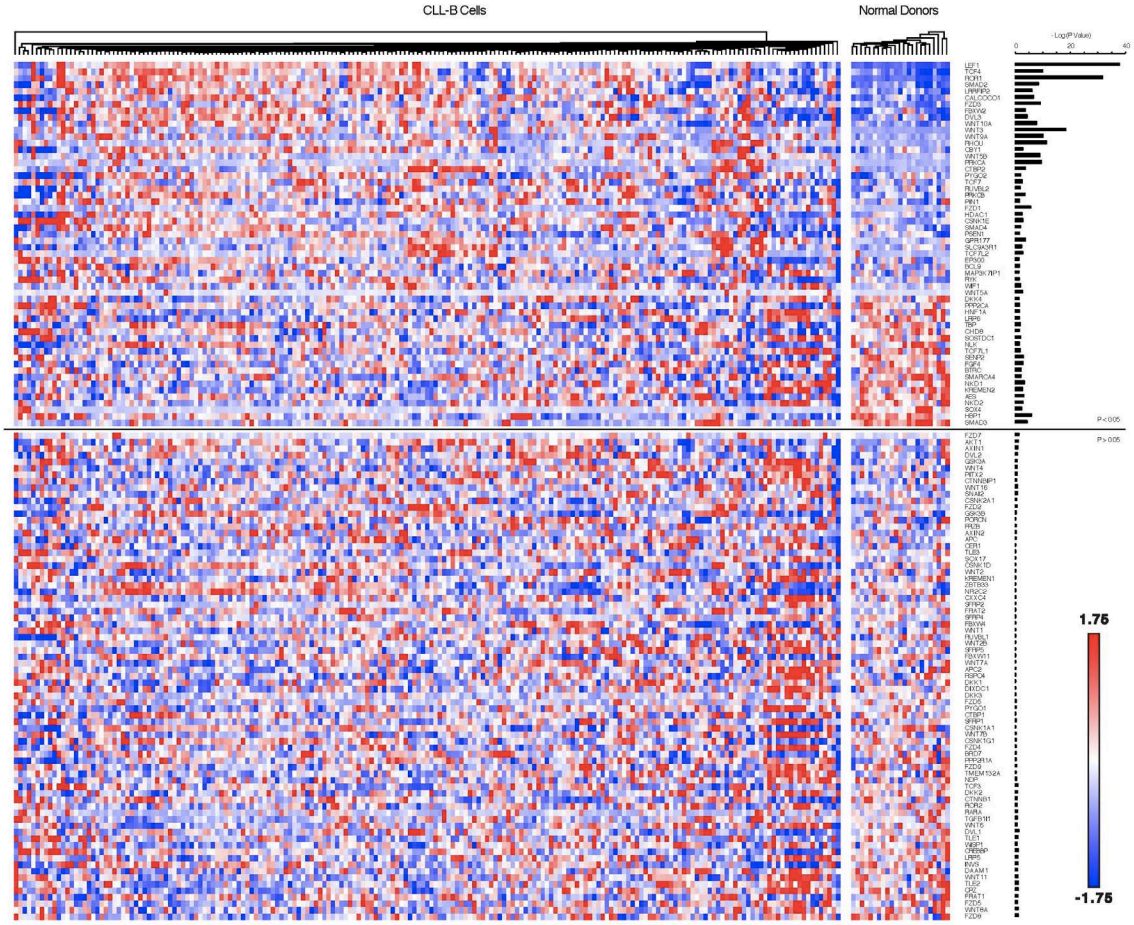

Figure S14. CLL-B cells show global Wnt pathway dysregulation absent of clear structure. Expression profiles for 131 Wnt pathway members in 193 CLL-B cells and 23 normal CD19+ B cells. Note that *LEF1* (top) is the most significantly dysregulated Wnt pathway member (upregulated).

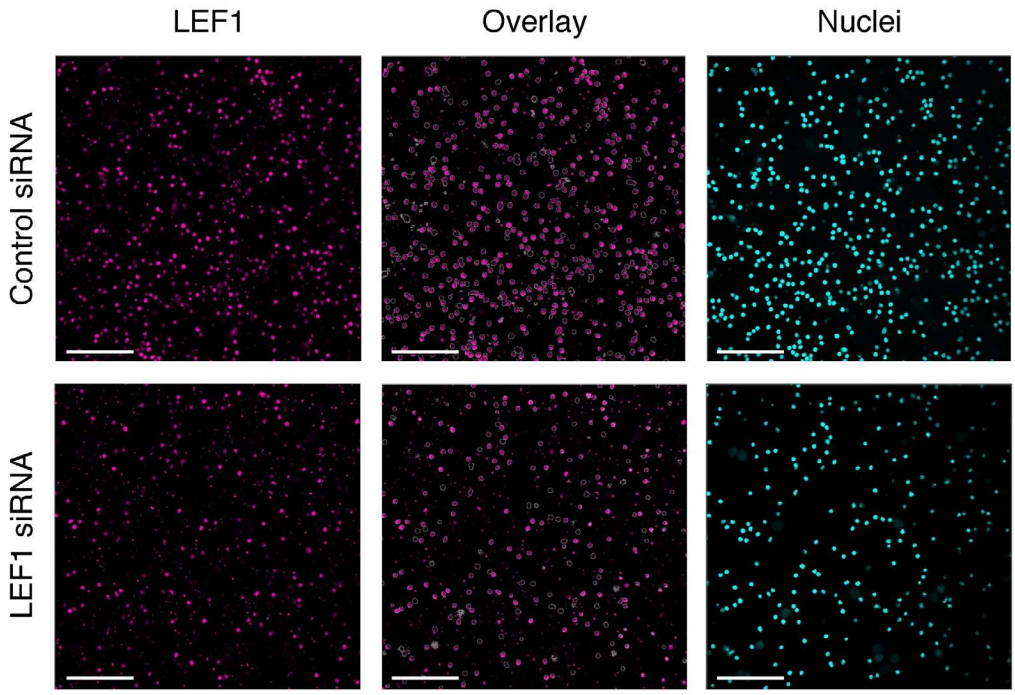

Figure S15. Knockdown of *LEF1* results in reduced protein expression and, in some patients, reduced cell viability.

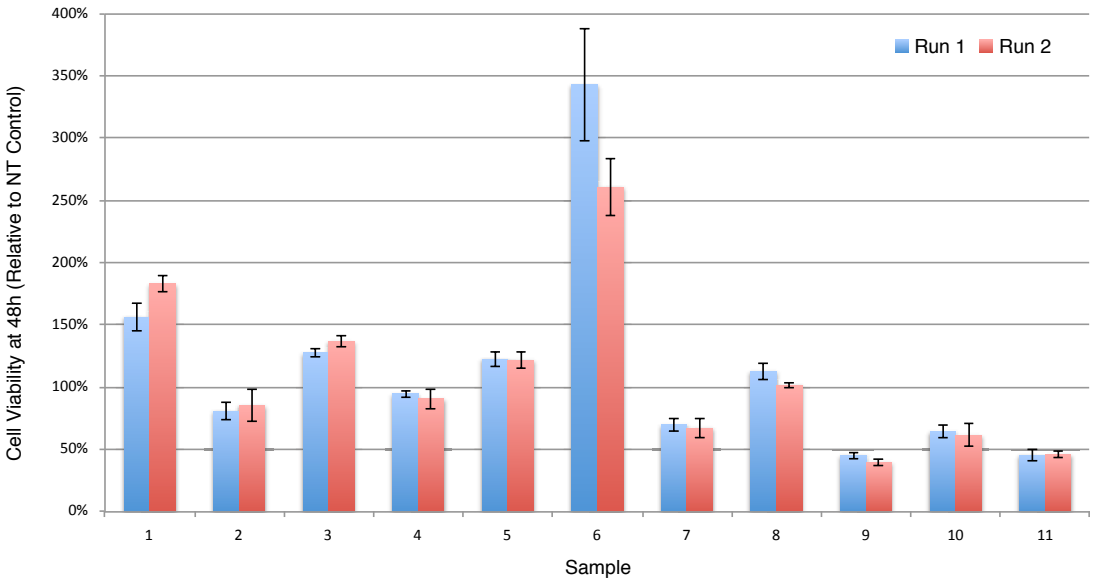

Figure S16. Reproducibility of the effect of *LEF1* knockdown on CLL-B cell viability. Shown is data (n = 3, mean ± standard error) for two independent knockdown experiments performed on 11 different patient samples.

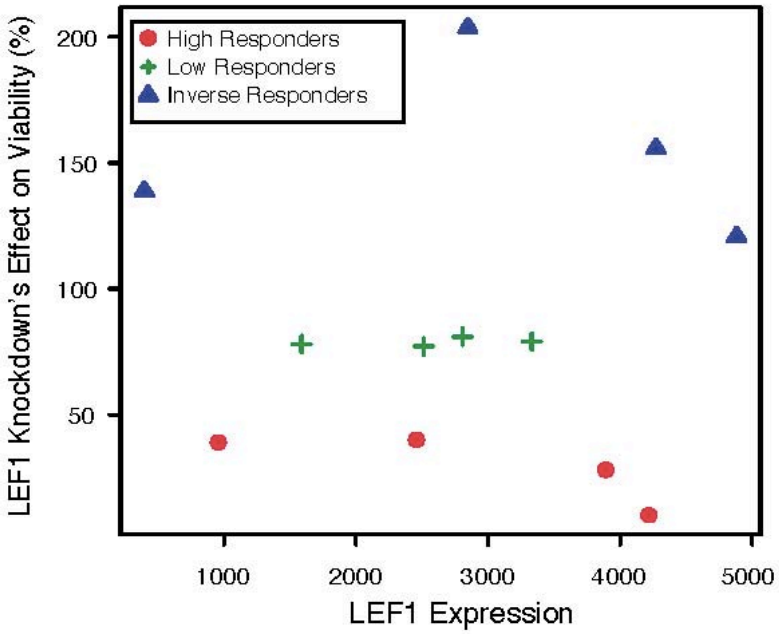

Figure S17. CLL sample *LEF1* expression does not correlate with magnitude of effect on sample viability following *LEF1* knockdown.

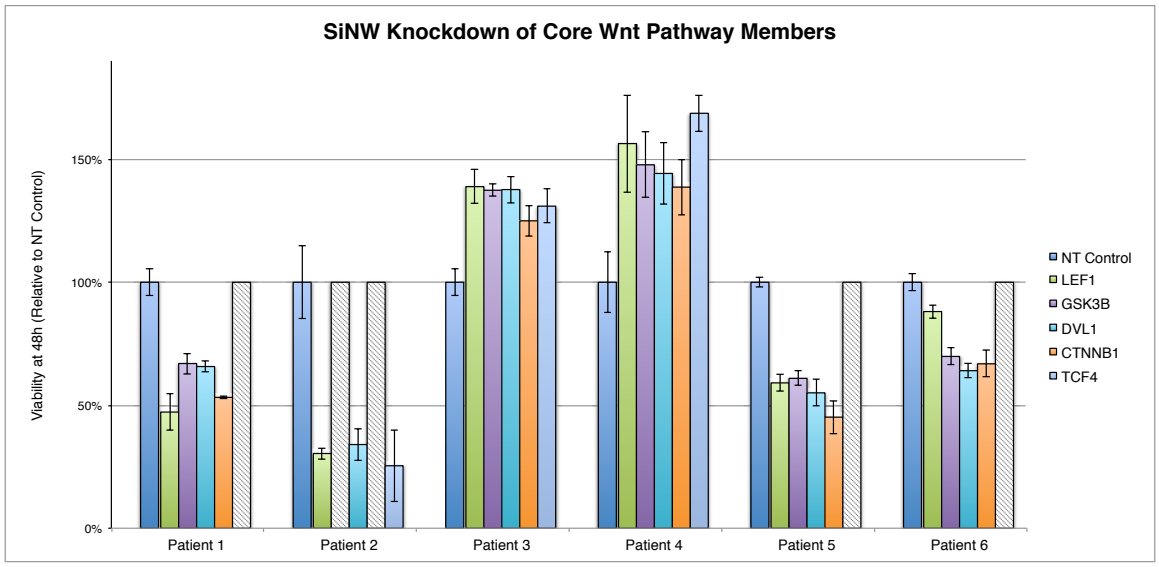

Figure S18. Although different patients show heterogeneous responses to knocking down *LEF1,* knocking down different core Wnt pathway members in same patient samples alters CLL-B cell viability in a similar fashion. All bars represent mean ± standard error (n = 3). Grey hashed bars equal to unity indicate that a given siRNA not tested on the particular sample.

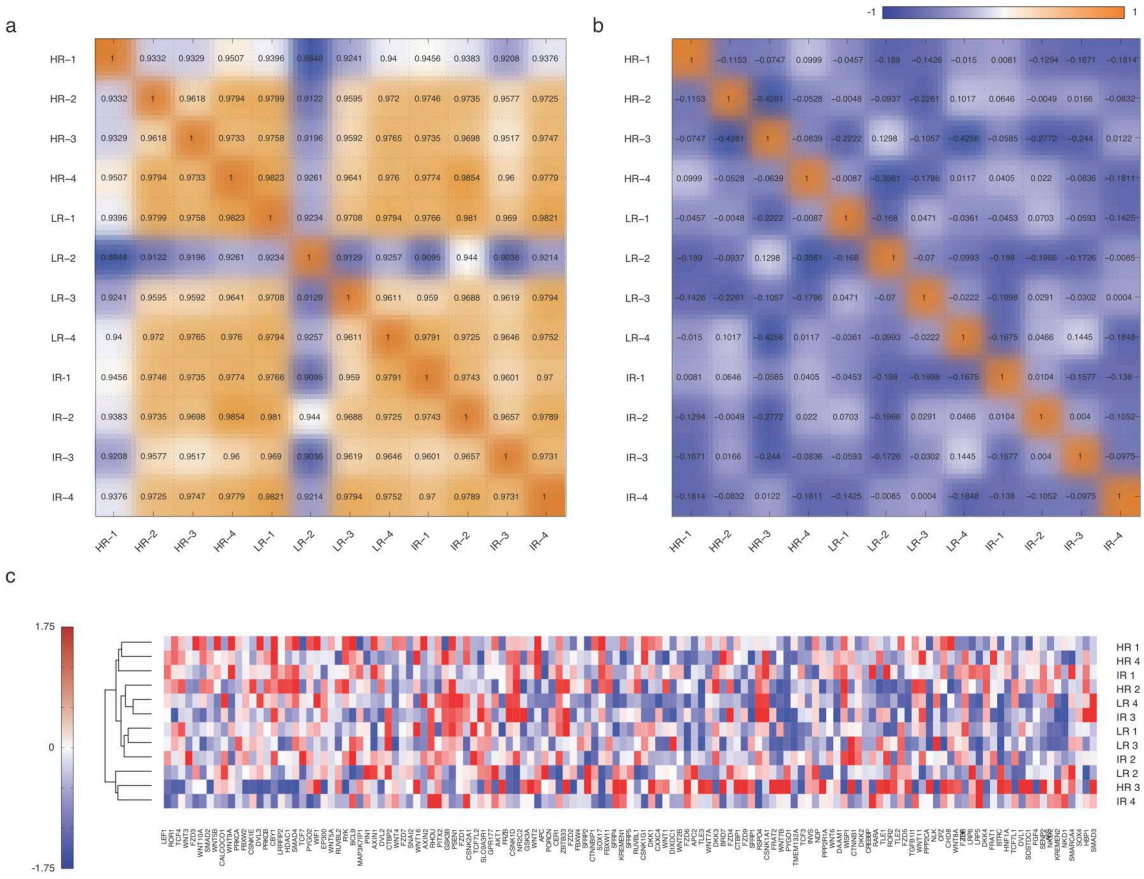

Figure S19. The functional sample groupings are not uncovered by correlations based on expression levels – unaltered (a) or z-scored (b) – nor by clustering across Wnt pathway members (**c**, identified using GSEA, (x-axis)).

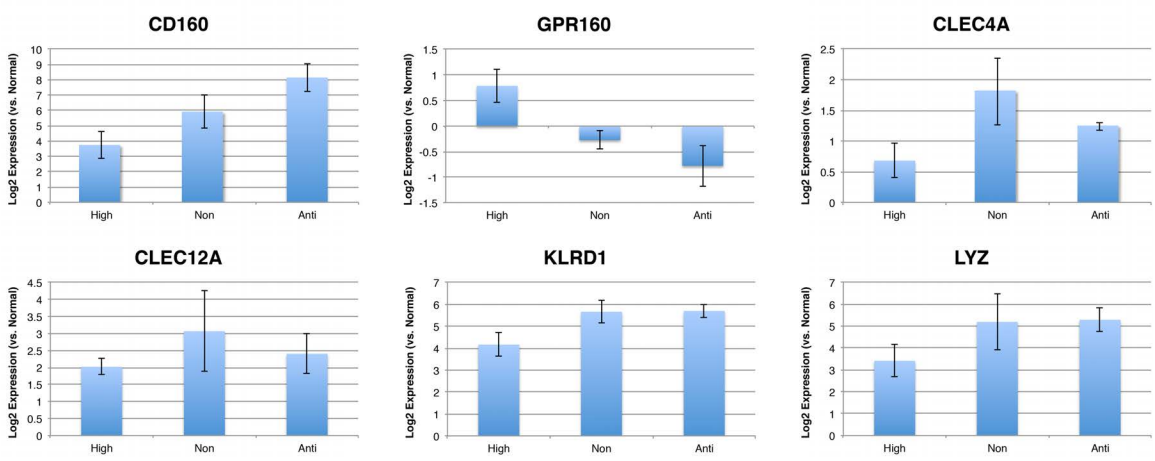

Figure S20. Microarray expression differences could be re-created for the few genes that were tested using qPCR.

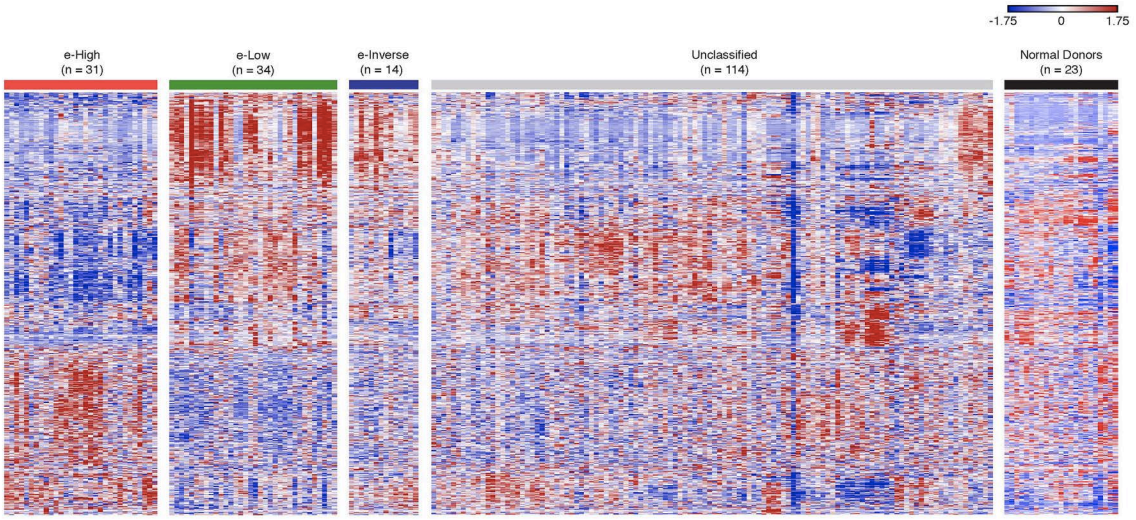

Figure S21. Clustering of all 193 CLL-B cell samples for which microarray data was available including unclassified samples across the 823 ANOVA identified genes. In the unclassified samples (grey bar), one additional major pattern emerged, reading, from top to bottom, blue, red, red. Profiles of normal donors (n = 23) (black bar) are shown in the rightmost grouping.

a

	e-High	e-Low	e-Inverse	P-Value
Patient Number	31 (39%)	34 (43%)	14 (18%)	
Treatment Status at Sample				
Treated	21 (70%)	17 (50%)	1 (7%)	0.00
IGHV				
Mutated	11 (41%)	16 (62%)	7 (70%)	0.17
ZAP-70				
Positive	15 (54%)	10 (40%)	3 (25%)	0.23
FISH Cytogenetics				
Del (13q-) Hetero	23 (82%)	16 (59%)	12 (86%)	0.10
Del (13q-) Homo	2 (7%)	6 (22%)	1 (7%)	0.33
Trisomy 12	2 (7%)	6 (22%)	0 (0%)	0.09
Del (11q)	6 (22%)	2 (8%)	1 (8%)	0.33
Del (17p)	6 (22%)	4 (15%)	1 (7%)	0.85

b

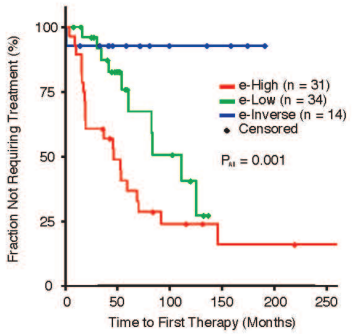

Figure S22. The extended ('e-') groups do not show enrichment for any known CLL cytogenetic markers[13, 18], but do show significantly different TTFTs. (a) Available clinical characteristics for the extended patient groups showing the absence of differences in standard cytogenetic markers (See Table S3). (b) Kaplan-Meier curves for the extended patient groups.

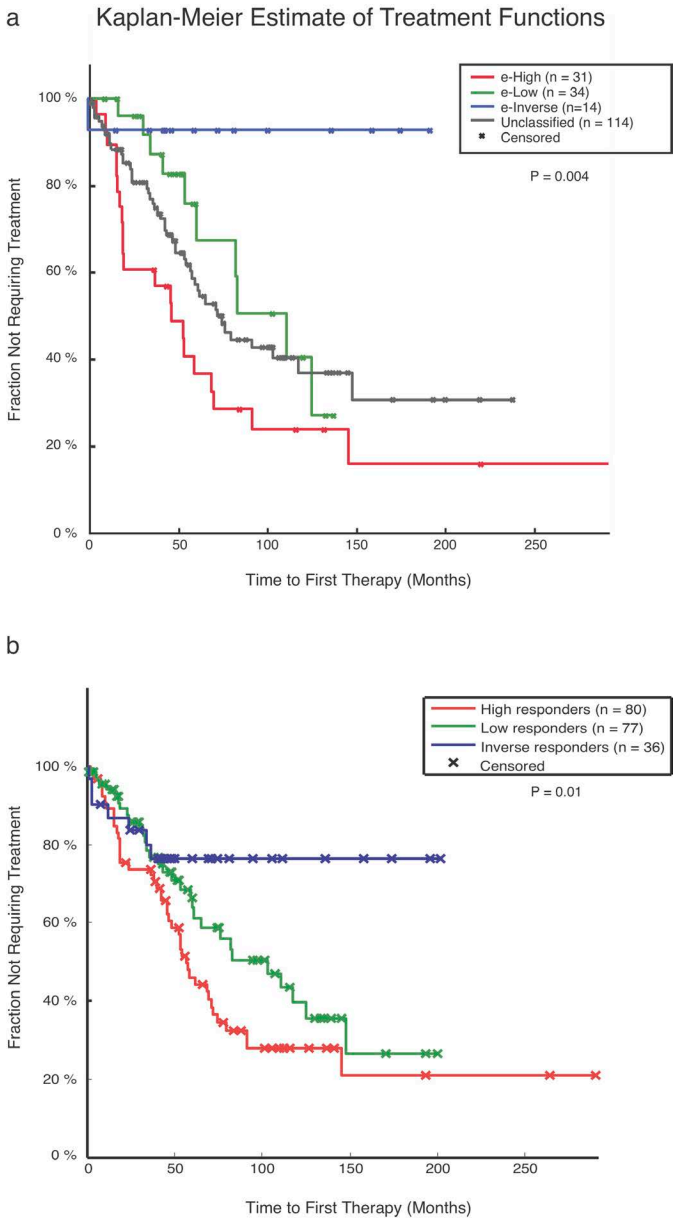

Figure S23. Different extended response groups show significantly different TTFTs. (a) Kaplan-Meier plot of all 193 patients for which Microarray data was available clustered according to our gene signature, including the unclassified patients (p = 0.004, Logrank test). (b) Kaplan-Meier plot with all patients classified using less stringent correlation criteria (p = 0.01, Logrank test).

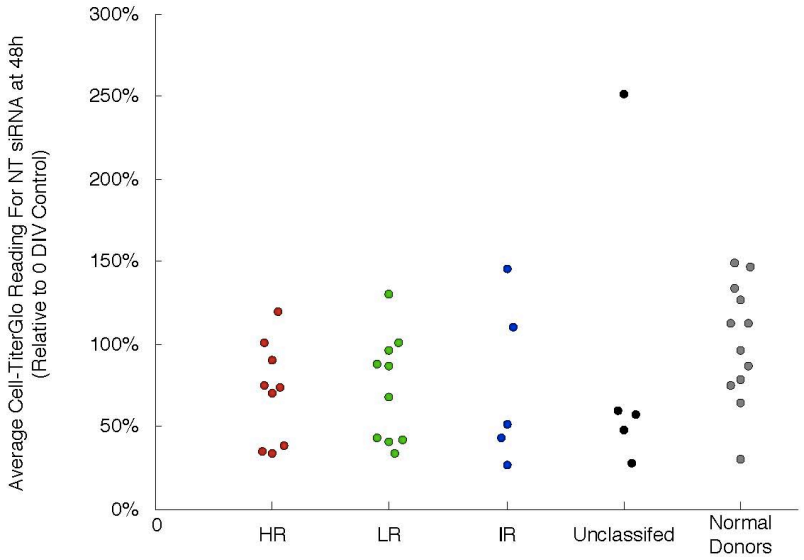

Figure S24. Average viability of NT siRNA control samples for Normal and CLL-B cells at 48 hours, plotted as a function of class. Differences in mean viability are not significant (p=0.53, One-Way ANOVA; p = 0.29, Kruskal-Wallis One-Way ANOVA).

References

1. Shalek, A. K.; Robinson, J. T.; Karp, E. S.; Lee, J. S.; Ahn, D.-R.; Yoon, M.-H.; Sutton, A.; Jorgolli, M.; Gertner, R. S.; Gujral, T. S.; Macbeath, G.; Yang, E. G.; Park, H. *Proc Natl Acad Sci U S A* **2010,** 107, (5), 1870-1875.

2. Chevrier, N.; Mertins, P.; Artyomov, M. N.; Shalek, A. K.; Iannacone, M.; Ciaccio, M. F.; Gat-Viks, I.; Tonti, E.; DeGrace, M. M.; Clauser, K. R.; Garber, M.; Eisenhaure, T. M.; Yosef, N.; Robinson, J.; Sutton, A.; Andersen, M. S.; Root, D. E.; von Andrian, U.; Jones, R. B.; Park, H.; Carr, S. A.; Regev, A.; Amit, I.; Hacohen, N. *Cell* **2011,** 147, (4), 853-867.

3. Wang, L.; Lawrence, M. S.; Wan, Y.; Stojanov, P.; Sougnez, C.; Stevenson, K.; Werner, L.; Sivachenko, A.; DeLuca, D. S.; Zhang, L.; Zhang, W.; Vartanov, A. R.; Fernandes, S. M.; Goldstein, N. R.; Folco, E. G.; Cibulskis, K.; Tesar, B.; Sievers, Q. L.; Shefler, E.; Gabriel, S.; Hacohen, N.; Reed, R.; Meyerson, M.; Golub, T. R.; Lander, E. S.; Neuberg, D.; Brown, J. R.; Getz, G.; Wu, C. J. *N Engl J Med* **2011,** 365, (26), 2497-2506.

4. Amit, I.; Garber, M.; Chevrier, N.; Leite, A. P.; Donner, Y.; Eisenhaure, T.; Guttman, M.; Grenier, J. K.; Li, W.; Zuk, O.; Schubert, L. A.; Birditt, B.; Shay, T.; Goren, A.; Zhang, X.; Smith, Z.; Deering, R.; McDonald, R. C.; Cabili, M.; Bernstein, B. E.; Rinn, J. L.; Meissner, A.; Root, D. E.; Hacohen, N.; Regev, A. *Science* **2009,** 326, (5950), 257-263.

5. Geiss, G.; Bumgarner, R.; Birditt, B.; Dahl, T.; Dowidar, N.; Dunaway, D.; Fell, H.; Ferree, S.; George, R.; Grogan, T. *Nat. Biotechnol.* **2008,** 26, (3), 317-325.

6. Irizarry, R. A.; Hobbs, B.; Collin, F.; Beazer-Barclay, Y. D.; Antonellis, K. J.; Scherf, U.; Speed, T. P. *Biostatistics* **2003,** 4, (2), 249-264.

7. Reich, M.; Liefeld, T.; Gould, J.; Lerner, J.; Tamayo, P.; Mesirov, J. P. *Nat. Genet.* **2006,** 38, (5), 500-501.

8. Johnson, W. E.; Li, C.; Rabinovic, A. *Biostatistics* **2007,** 8, (1), 118-127.

9. Angers, S.; Moon, R. T. *Nat. Rev. Mol. Cell Bio.* **2009,** 10, (7), 468-477.

10. Klaus, A.; Birchmeier, W. *Nat. Rev. Cancer* **2008,** 8, (5), 387-398.

11. Mosimann, C.; Hausmann, G.; Basler, K. *Nat. Rev. Mol. Cell Biol.* **2009,** 10, (4), 276-286.

12. Huang, D. W.; Sherman, B. T.; Lempicki, R. A. *Nucleic Acids Res.* **2009,** 37, (1), 1-13.

13. Huang, D. W.; Sherman, B. T.; Lempicki, R. A. *Nat. Protoc.* **2009,** 4, (1), 44-57.

14. Zenz, T.; Mertens, D.; Küppers, R.; Döhner, H.; Stilgenbauer, S. *Nat. Rev. Cancer* **2010,** 10, (1), 37-50.

15. Barbie, D. A.; Tamayo, P.; Boehm, J. S.; Kim, S. Y.; Moody, S. E.; Dunn, I. F.; Schinzel, A. C.; Sandy, P.; Meylan, E.; Scholl, C.; Fröhling, S.; Chan, E. M.; Sos, M. L.; Michel, K.; Mermel, C.; Silver, S. J.; Weir, B. A.; Reiling, J. H.; Sheng, Q.; Gupta, P. B.; Wadlow, R. C.; Le, H.; Hoersch, S.; Wittner, B. S.; Ramaswamy, S.; Livingston, D. M.; Sabatini, D. M.; Meyerson, M.; Thomas, R. K.; Lander, E. S.; Mesirov, J. P.; Root, D. E.; Gilliland, D. G.; Jacks, T.; Hahn, W. C. *Nature* **2009,** 462, (7269), 108-112.

16. Kim, J.; Woo, A. J.; Chu, J.; Snow, J. W.; Fujiwara, Y.; Kim, C. G.; Cantor, A. B.; Orkin, S. H. *Cell* **2010,** 143, (2), 313-324.

17. Marson, A.; Levine, S. S.; Cole, M. F.; Frampton, G. M.; Brambrink, T.; Johnstone, S.; Guenther, M. G.; Johnston, W. K.; Wernig, M.; Newman, J.; Calabrese, J. M.; Dennis, L. M.; Volkert, T. L.; Gupta, S.; Love, J.; Hannett, N.; Sharp, P. A.; Bartel, D. P.; Jaenisch, R.; Young, R. A. *Cell* **2008,** 134, (3), 521-533.

18. Ben-Porath, I.; Thomson, M. W.; Carey, V. J.; Ge, R.; Bell, G. W.; Regev, A.; Weinberg, R. A. *Nat. Genet.* **2008,** 40, (5), 499-507.